NANOPHOTONICS

Chaos-assisted broadband momentum transformation in optical microresonators

Xuefeng Jiang,[1,2,3]* Linbo Shao,[4]* Shu-Xin Zhang,[1,2] Xu Yi,[5] Jan Wiersig,[6] Li Wang,[1,2] Qihuang Gong,[1,2,7] Marko Lončar,[4] Lan Yang,[3] Yun-Feng Xiao[1,2,7]†

The law of momentum conservation rules out many desired processes in optical microresonators. We report broadband momentum transformations of light in asymmetric whispering gallery microresonators. Assisted by chaotic motions, broadband light can travel between optical modes with different angular momenta within a few picoseconds. Efficient coupling from visible to near-infrared bands is demonstrated between a nanowaveguide and whispering gallery modes with quality factors exceeding 10 million. The broadband momentum transformation enhances the device conversion efficiency of the third-harmonic generation by greater than three orders of magnitude over the conventional evanescent-wave coupling. The observed broadband and fast momentum transformation could promote applications such as multicolor lasers, broadband memories, and multiwavelength optical networks.

Conservation of momentum, as a fundamental law of nature, states that the momentum of a system does not change with time evolution in classical or quantum isolated systems. In optics and photonics, this conservation law regulates many interesting physical processes (*1*), such as frequency conversions (*2*–*6*), frequency combs (*7*, *8*), metamaterials (*9*), and optical cross-talk in qubits (*10*). Optical microresonators promote a wide range of such processes by storing and manipulating light in a small volume (*11*), but efficient coupling has become an important prerequisite for leveraging high–quality (*Q*) factors of microresonators. A momentum-conserved way to directly access the highly confined resonant modes is the evanescent-wave coupling. Although this ensures the coupling efficiency at specific wavelengths, it limits the coupling bandwidth and restricts optical resonators from broadband applications.

Efficient evanescent-wave coupling requires that the phase velocities, i.e., momenta, of the modes be supported by a coupler [e.g., prism (*12*, *13*) or waveguide (*14*–*19*)] to match those of a microresonator—known as the phase-matching condition. This can be accomplished by engineering the size of a waveguide coupler or carefully controlling the incident angle of light in the case of a prism. Because the phase velocity in a photonic device is affected by both material and geometry dispersion of the device, the optical modes of the coupler and the resonator can have different wavelength dependence. As a result, even if the phase-matching condition is satisfied at a particular wavelength band, it is unlikely to ensure phase matching in a spectral window far away from the initial band, making it challenging to maintain high coupling efficiencies over a wide wavelength range. Scattering-based coupling (e.g., grating, notch, and nanoparticle) provides another way to access optical resonances but suffers narrow bandwidth (*20*, *21*), *Q* factor spoiling (*22*), or low coupling efficiency (*23*, *24*).

Here we realize the broadband and fast momentum transformation in optical microresonators, which achieves efficient coupling to ultrahigh-*Q* whispering gallery modes (WGMs) over two octave frequencies. An asymmetric (deformed) microresonator (*25*–*27*) is utilized to create chaotic channels that transform momenta of light. Consequently, through dynamic tunneling (*25*, *28*–*31*), such chaotic channels can serve as a liaison to connect light in the external couplers and the high-*Q* WGMs, by lifting and lowering the angular momenta of light between them. In the experiment, broadband momentum transformation has been demonstrated for simultaneous coupling from visible band to near infrared between an externally guided mode and WGMs with *Q* factors greater than 10^7.

A deformed microtoroid is side coupled with an optical subwavelength-sized nanowaveguide (Fig. 1A). The small deformation introduces chaotic modes, which guide the light in the microresonator with a chaotic trajectory. Because of the chaotic motion, the angular momentum of light is not conserved, and it changes with time, covering a broad range of values. By designing the shape of the microresonator appropriately (*32*), specific chaotic channels are created to transform angular momenta between waveguide modes and WGMs (Fig. 1B). When the angular momentum of light in the chaotic channel approaches that of WGMs, the efficient coupling can be achieved through dynamic tunneling. The small dispersion of the nanowaveguide helps to optimize the wavelength-independent refraction between the chaotic channel and the waveguide modes (*32*). This process is independent of the phase-matching condition between the waveguide modes and WGMs.

The results of full three-dimensional finite-difference time-domain (3D FDTD) simulation

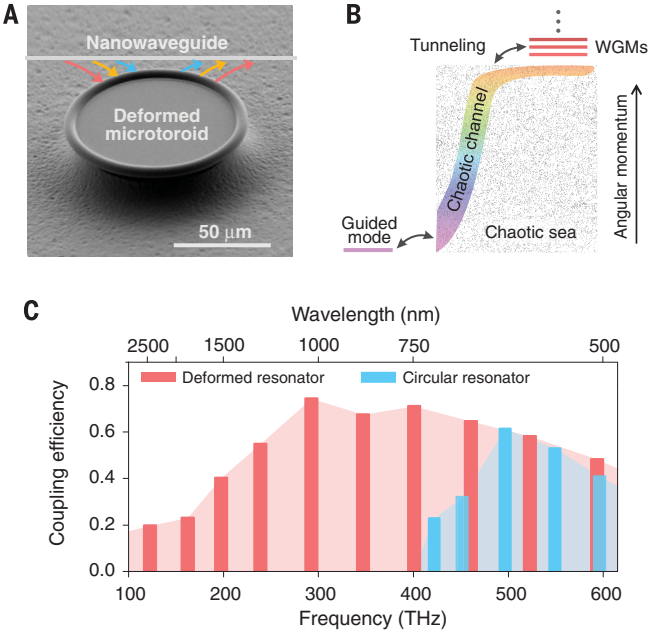

Fig. 1. Schematic of broadband momentum transformation in an optical microresonator. (**A**) A scanning electron microscope image of a deformed microresonator coupled with an optical nanowaveguide. (**B**) Schematic for the chaos-assisted momentum transformation–enabled broadband coupling process. The vertical axis represents the angular momentum in the resonator. The waveguide modes and the WGMs are coupled to the chaotic channels, separately. (**C**) 3D FDTD simulation showing coupling efficiencies of a deformed (red) and a circular (blue) microresonator coupled with a nanowaveguide.

[1]State Key Laboratory for Mesoscopic Physics and School of Physics, Peking University, Beijing 100871, China. [2]Collaborative Innovation Center of Quantum Matter, Beijing 100871, China. [3]Department of Electrical and Systems Engineering, Washington University, St. Louis, MO 63130, USA. [4]John A. Paulson School of Engineering and Applied Science, Harvard University, Cambridge, MA 02138, USA. [5]T. J. Watson Laboratory of Applied Physics, California Institute of Technology, Pasadena, CA 91125, USA. [6]Institut für Theoretische Physik, Otto-von-Guericke-Universität Magdeburg, Postfach 4120, 39016 Magdeburg, Germany. [7]Collaborative Innovation Center of Extreme Optics, Taiyuan, Shanxi 030006, China.
*These authors contributed equally to this work. †**Corresponding author. Email: yfxiao@pku.edu.cn**

(Fig. 1C) demonstrate that this momentum transformation enables coupling bandwidth greater than two octaves, spanning from 120 to 600 THz in frequency (500 to 2500 nm in wavelength). In the simulation, the principal and minor diameters of the microtoroidal resonator are set to 24 and 4 μm, respectively. The resonators are contacted and coupled to a tapered silica-fiber waveguide with a diameter of 0.5 μm. The deformation of the microresonator is about 4%, as defined by the difference of diameters at various angles over the largest principal diameter (*32*). In the simulation, we keep the *Q* factor constant, which is achieved by adding a value of 5×10^{-5} to the imaginary part of the material refractive index. The coupling efficiency is derived from the transmission of the nanowaveguide. The coupling efficiencies of WGMs in deformed and circular resonators from visible to near-infrared bands (Fig. 1C) show that the momentum transformation in the microresonator pushes the lower (higher) bound of the frequency (wavelength) from 420 to 120 THz (715 to 2500 nm), giving the coupling bandwidth a threefold (eightfold) enhancement in frequency (wavelength).

The dynamics of the momentum transformation is investigated by the short-time Fourier transforms in 3D FDTD simulation, through which the electromagnetic (EM) field at a resonant frequency of a WGM can be identified. A short pulse of 10 fs with spectrum covering the WGM resonance (1516 nm) is used to excite the resonant modes; temporal EM fields in real space during the momentum transformation are recorded. As shown in Fig. 2, A to E; fig. S1; and movie S1, the EM fields at different times reveal the momentum-transformation process. To quantitatively explore the momentum transformation–enabled coupling process, the mode indices (blue curve in Fig. 2F) are calculated to infer the angular momentum of light (*32*). The WGM portions of the EM field (red curve in Fig. 2F), indicating the overall coupling, are calculated by projecting the short-time EM field to the stabilized fundamental WGM.

As shown in Fig. 2A, the pulse propagating along the waveguide enters the coupling region at 0.06 ps. The mode index is 1.07, given that the diameter of the waveguide (0.5 μm) is much smaller than the incident light wavelength (~1.5 μm). From 0.06 to 1.0 ps, the light is coupled into the chaotic channels with a low mode index from the waveguide (Fig. 2B). As the chaos evolves (Fig. 2, B and C), it elevates the mode index from 1.07 to 1.41 (inset of Fig. 2F), which is close to that of the WGMs. This means that in a properly designed resonator, the chaotic motion efficiently transforms the angular momentum of light from the externally propagating mode to WGMs within a few picoseconds, or a few circular rounds as the light travels in the resonator. From 1 to 50 ps, the light dynamically tunnels into a WGM from the chaotic channel as the WGM portion of the field increases over time. Meanwhile, the mode index remains almost unchanged after 1 ps, confirming that the excitation of the WGM occurs through the neighboring chaotic modes instead of the waveguide with low mode index. At 20 ps, around half of the energy of the EM fields is attributable to the WGM, and the mixing of chaotic mode and the WGM is apparent in Fig. 2D. At 50 ps, about 90% of the EM field inside the resonator is attributable to the WGM. After 50 ps, the WGM portion of the EM field slowly increases with small fluctuations. At 200 ps (Fig. 2E), only the WGM survives as a result of its long lifetime (small decay rate) (*32*).

It should be noted that the trajectory of light in the chaotic channel is controlled by the resonator shape; the mode indices of most of the light increases within the first few rounds of its chaotic motion (inset, Fig. 2F). The light in the chaotic channel with high mode index dynamically tunnels into the WGM, as the field projection to the WGM increases with time (Fig. 2F). We can see that the dynamic tunneling process is much slower than the momentum elevation of the chaotic modes. The time evolution of the WGM portion reveals this dynamic tunneling process. To understand the coupling process, we model the coupling between in-resonator chaos and a WGM by a two-level system (*32*) and fit the WGM portions to the model in Fig. 2F. Given the decay rate of a high-*Q* WGM (chaotic mode) γ_m (γ_c) and tunneling rate κ, the maximum slope of the WGM portion is approximately given by $\dot{\eta}_{max} = \frac{1}{4}(\gamma_c - \gamma_m) + \frac{\kappa^2}{\gamma_c - \gamma_m}$, where $\gamma_c - \gamma_m > 2\kappa$ is assumed.

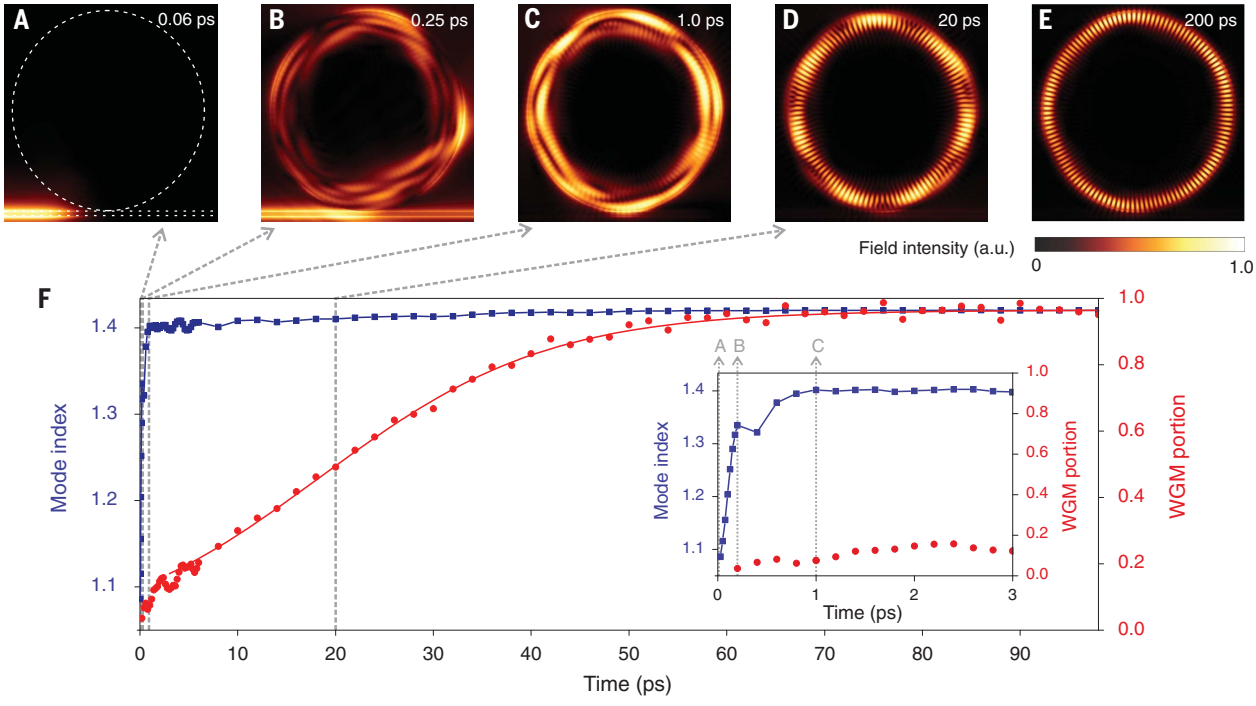

Fig. 2. Transient dynamic process of the momentum transformation–enabled efficient coupling. (**A** to **E**) Short-time snapshots in 3D FDTD simulations of spatial-field intensity distribution with a 10-fs duration pulse coupled into the resonator through the nanowaveguide. (A) A short pulse propagating in the waveguide. White dashed lines mark the geometric boundaries of the nanowaveguide and the microresonator. (B) The light being refracted into the chaotic channel of the microresonator. (C) The chaotic motion of light. (D) Dynamic tunneling of light into a WGM. (E) The established WGM. (**F**) Temporal evolution of mode index (blue) and excited WGM portion (red dots) derived from spatial intensity distribution, and the theoretical WGM portion (red curve) derived from the two-level model. Inset shows a zoom-in of the mode index (blue) and WGM portion (red dots) in the first 3 ps, with labels A, B, and C indicating the moments at 0.06 ps (A), 0.25 ps (B), and 1 ps (C).

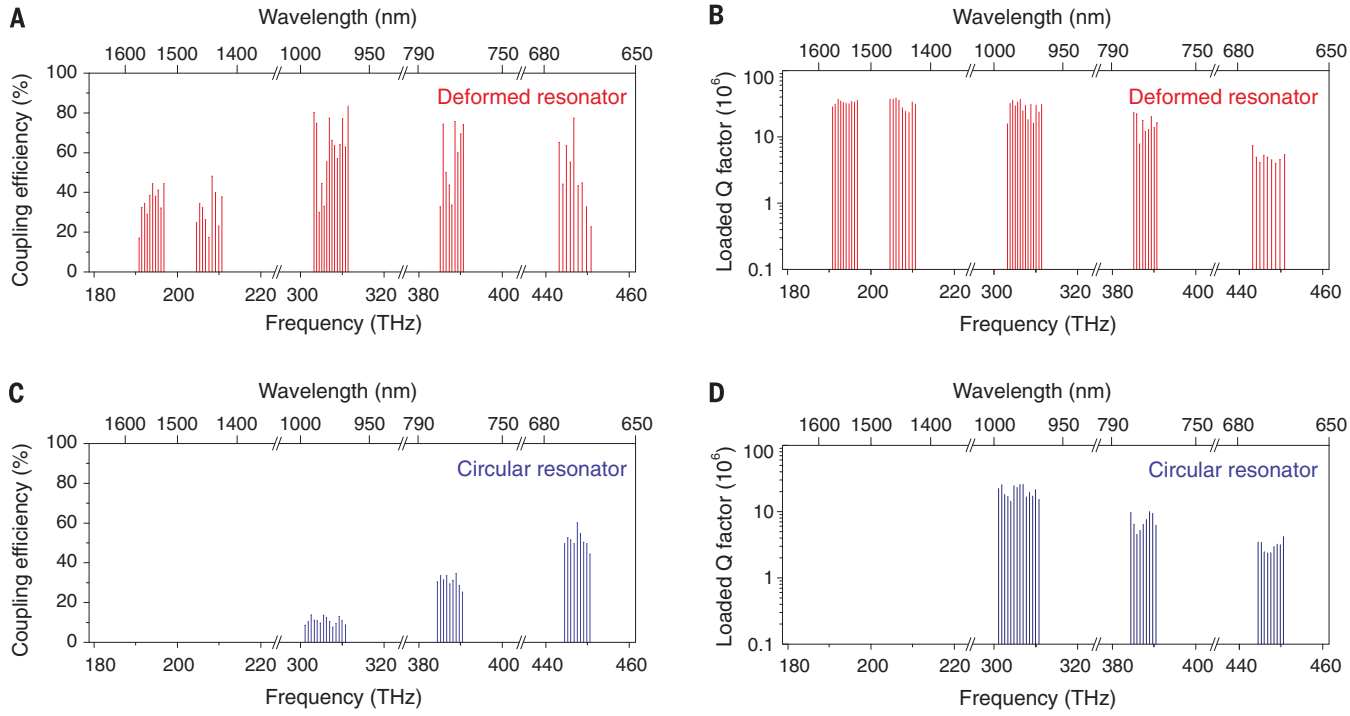

Fig. 3. Experimental results of momentum transformation–enabled broadband coupling. Deformed (**A** and **B**) and circular (**C** and **D**) resonators coupled by a nanowaveguide with a diameter of about 0.5 μm, with their respective coupling efficiencies (A) and (C) and loaded *Q* factors (B) and (D) shown. The measurements are performed in 670-, 770-, 980-, 1450-, and 1550-nm wavelength bands. In 1450- and 1550-nm bands, no high-*Q* mode of the circular resonator is identified in the transmission spectra.

Experimentally, we use monolithic silica deformed microtoroids with a principal diameter of 80 μm and a minor diameter of about 6 μm (*32*). A tapered fiber waveguide with a diameter of about 0.5 μm is used to excite the WGMs and also to collect the transmission (Fig. 3, A and B); for comparison, a circular microtoroid with almost the same principal and minor diameters is used as a reference resonator (Fig. 3, C and D). The transmissions over a broad wavelength range are measured by five tunable lasers at 670-, 770-, 980-, 1450-, and 1550-nm wavelength bands. Compared to its circular counterpart, the loaded *Q* factors of the deformed resonator are not appreciably lowered in any measured wavelength band and exceed 10^7 from 750 to 1600 nm. The deterioration of *Q* factors at shorter wavelength might be caused by additional coupling loss introduced by the direct evanescent-wave coupling. The coupling efficiencies for the deformed resonator exceed 50% from 650 to 1000 nm and maintain 30% near 1550 nm. Efficiencies decrease at longer wavelengths because light is less confined in the nanowaveguide. Coupling to high-*Q* factor modes in the circular resonator is not observed at any wavelength longer than 1000 nm by using the same nanowaveguide, whereas the existence of the high–*Q* factor modes is separately confirmed by using corresponding phase-matched waveguides at these wavelengths. A coupling bandwidth greater than 900 nm (limited by the availability of tunable lasers) is measured for the deformed resonator, whereas the coupling bandwidth is only 300 nm for its circular counterpart. This observation indicates that the chaotic channel in the deformed resonator at least triples the coupling bandwidth.

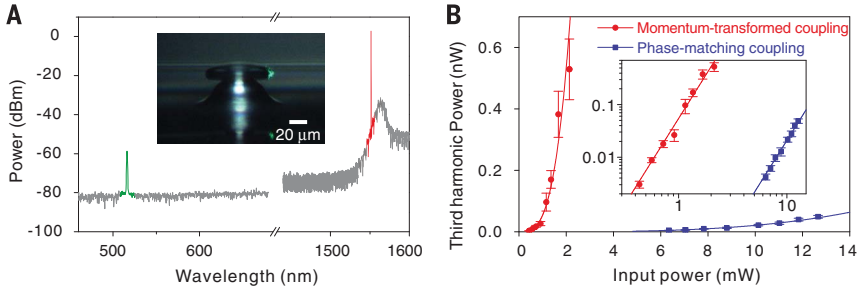

Fig. 4. Third-harmonic generation experiment. (**A**) THG spectrum in a deformed microresonator collected by a single nanowaveguide with a pump power of about 4.37 mW. Red and green colors highlight the pump and THG wavelengths, respectively. Inset shows a side-view photograph of the resonator emitting THG green light. dBm, decible relative to a milliwatt. (**B**) Measured THG power of the same deformed resonator by the chaos-assisted momentum-transformed coupling and the direct phase-matching coupling as a function of the pump power.

As an application of the momentum transformation in microresonators, we demonstrate third-harmonic generation (THG) with the device conversion efficiency enhanced by greater than three orders of magnitude. To minimize other factors, one deformed microtoroid is used under two coupling conditions: (i) momentum transformation–enabled coupling with a tapered fiber nanowaveguide and (ii) direct phase-matching coupling near 1550 nm using a tapered fiber with a diameter of about 1.5 μm. Also, the same optical modes are used in both coupling schemes. The pump mode is at 1551.4 nm with intrinsic *Q* factor of 7.0×10^7, and the third-harmonic mode occurs at 517.1 nm (Fig. 4A). In both cases, a bright green light (of THG wavelength) is visible from the camera (inset, Fig. 4A). However, the externally collected intensity of THG light is much greater using this momentum transformation–enabled coupling. As expected, the output-input power relations of THG for both cases (Fig. 4B) show a cubic relationship. The momentum transformation–enabled scheme improves the device conversion efficiency of THG by about 5000-fold in comparison with the direct phase-matching coupling (*32*).

We envision that the present broadband momentum transformation in optical microresonators provides a feasible and efficient method for

accessing and networking high-Q optical resonant modes. The chaotic channels bridge the huge gap in light angular momentum, which makes efficient coupling possible between optical devices with different refractive indices—such as lithium niobate, diamond, silicon, and gallium arsenide—over a broadband wavelength range. This chaos-assisted momentum-transformation mechanism can also be widely extended to various photonics applications, such as cascaded Raman lasing (*32*), and frequency comb generation.

REFERENCES AND NOTES

1. A. Imamoğlu, H. Schmidt, G. Woods, M. Deutsch, *Phys. Rev. Lett.* **79**, 1467–1470 (1997).
2. T. Carmon, K. J. Vahala, *Nat. Phys.* **3**, 430–435 (2007).
3. R. W. Andrews *et al.*, *Nat. Phys.* **10**, 321–326 (2014).
4. A. Rueda *et al.*, *Optica* **3**, 597 (2016).
5. C. Dong, V. Fiore, M. C. Kuzyk, H. Wang, *Science* **338**, 1609–1613 (2012).
6. J. T. Hill, A. H. Safavi-Naeini, J. Chan, O. Painter, *Nat. Commun.* **3**, 1196 (2012).
7. T. J. Kippenberg, R. Holzwarth, S. A. Diddams, *Science* **332**, 555–559 (2011).
8. T. Herr *et al.*, *Nat. Photonics* **8**, 145–152 (2014).
9. N. Yu *et al.*, *Science* **334**, 333–337 (2011).
10. C. Monroe, J. Kim, *Science* **339**, 1164–1169 (2013).
11. K. J. Vahala, *Nature* **424**, 839–846 (2003).
12. V. Sandoghdar *et al.*, *Phys. Rev. A* **54**, R1777–R1780 (1996).
13. A. Mazzei, S. Götzinger, L. S. Menezes, V. Sandoghdar, O. Benson, *Opt. Commun.* **250**, 428–433 (2005).
14. D. R. Rowland, J. D. Love, *IEE Proc. J Optoelectron.* **140**, 177–188 (1993).
15. J. C. Knight, G. Cheung, F. Jacques, T. A. Birks, *Opt. Lett.* **22**, 1129–1131 (1997).
16. M. Cai, O. Painter, K. J. Vahala, *Phys. Rev. Lett.* **85**, 74–77 (2000).
17. A. Yariv, *IEEE Photonics Technol. Lett.* **14**, 483–485 (2002).
18. T. Carmon, S. Y. Wang, E. P. Ostby, K. J. Vahala, *Opt. Express* **15**, 7677–7681 (2007).
19. K. Srinivasan, O. Painter, *Nature* **450**, 862–865 (2007).
20. D. C. Aveline, L. M. Baumgartel, G. Lin, N. Yu, *Opt. Lett.* **38**, 284–286 (2013).
21. V. Ilchenko, A. Savchenkov, L. Maleki, U.S. Patent 7929589 (2011).
22. Q. J. Wang *et al.*, *Proc. Natl. Acad. Sci. U.S.A.* **107**, 22407–22412 (2010).
23. Y. C. Liu *et al.*, *Phys. Rev. A* **85**, 013843 (2012).
24. J. Zhu *et al.*, *Sci. Rep.* **4**, 6396 (2014).
25. H. Cao, J. Wiersig, *Rev. Mod. Phys.* **87**, 61–111 (2015).
26. J. U. Nöckel, A. D. Stone, *Nature* **385**, 45–47 (1997).
27. C. Gmachl *et al.*, *Science* **280**, 1556–1564 (1998).
28. S. Lacey, H. Wang, D. H. Foster, J. U. Nöckel, *Phys. Rev. Lett.* **91**, 033902 (2003).
29. J. Yang *et al.*, *Phys. Rev. Lett.* **104**, 243601 (2010).
30. S. Shinohara *et al.*, *Phys. Rev. Lett.* **104**, 163902 (2010).
31. Q. Song, L. Ge, B. Redding, H. Cao, *Phys. Rev. Lett.* **108**, 243902 (2012).
32. Materials and methods are available as supplementary materials.

ACKNOWLEDGMENTS

We thank K. Vahala, H. Wang, C.-L. Zou, Q.-F. Yang, B. Shen, and M. Zhang for fruitful discussions. This project is supported by the National Key R and D Program of China (grant nos. 2016YFA0301302 and 2013CB328704) and the National Natural Science Foundation of China (grant nos. 61435001, 11474011, 11654003, and 11527901). L.Y. and X.J. acknowledge support from the NSF (grant no. DMR-1506620). L.S. is supported by the Center for Integrated Quantum Materials under the NSF (grant no. DMR-1231319). The simulations were run on the Odyssey cluster supported by the Faculty of Arts and Sciences Division of Science, Research Computing Group at Harvard University.

SUPPLEMENTARY MATERIALS

www.sciencemag.org/content/358/6361/344/suppl/DC1
Materials and Methods
Supplementary Text
Figs. S1 to S13
References (*33*–*52*)
Movie S1

12 June 2017; accepted 6 September 2017
10.1126/science.aao0763

Science

Chaos-assisted broadband momentum transformation in optical microresonators

Xuefeng Jiang, Linbo Shao, Shu-Xin Zhang, Xu Yi, Jan Wiersig, Li Wang, Qihuang Gong, Marko Loncar, Lan Yang and Yun-Feng Xiao

Science **358** (6361), 344-347.
DOI: 10.1126/science.aao0763

Harnessing chaos for enhanced coupling

Functional optical devices typically require the coupling of light between different components. However, conservation of momentum usually limits the bandwidth of the coupling, often to a near-resonant effect. Jiang *et al.* show that slightly deformed microring resonators might be able to relax those restrictions. The chaotic scattering of the light within the deformed structure can transform optical modes of different angular momenta within a few picoseconds, providing a promising route to develop advanced nanophotonic circuits and devices.

Science, this issue p. 344